
Modern Hopfield Networks for Few- and Zero-Shot Reaction Prediction

Philipp Seidl^{1,2} Philipp Renz^{1,2} Natalia Dyubankova³ Paulo Neves³ Jonas Verhoeven³ Jörg K. Wegner³
Sepp Hochreiter^{1,2,4} Günter Klambauer^{1,2}

Abstract

An essential step in the discovery of new drugs and materials is the synthesis of a molecule that exists so far only as an idea to test its biological and physical properties. While computer-aided design of virtual molecules has made large progress, computer-assisted synthesis planning (CASP) to realize physical molecules is still in its infancy and lacks a performance level that would enable large-scale molecule discovery. CASP supports the search for multi-step synthesis routes, which is very challenging due to high branching factors in each synthesis step and the hidden rules that govern the reactions. The central and repeatedly applied step in CASP is reaction prediction, for which machine learning methods yield the best performance. We propose a novel reaction prediction approach that uses a deep learning architecture with modern Hopfield networks (MHNs) that is optimized by contrastive learning. An MHN is an associative memory that can store and retrieve chemical reactions in each layer of a deep learning architecture. We show that our MHN contrastive learning approach enables few- and zero-shot learning for reaction prediction which, in contrast to previous methods, can deal with rare, single, or even no training example(s) for a reaction. On a well established benchmark, our MHN approach pushes the state-of-the-art performance up by a large margin as it improves the predictive top-100 accuracy from 0.858 ± 0.004 to 0.959 ± 0.004 . This advance might pave the way to large-scale molecule discovery.

1. Introduction

The design of a new molecule usually starts with the idea of a new chemical structure that is supposed to have desired

¹Institute for Machine Learning, Johannes Kepler University, Linz, Austria ²ELLIS Unit Linz ³Janssen Pharmaceutica ⁴IARAI. Correspondence to: Günter Klambauer <klambauer@ml.jku.at>.

properties (Lombardino & Lowe, 2004). In drug discovery, a desired property can be the inhibition of a disease or a virus and in material science, thermal stability. From the design idea of the molecule, a virtual molecule is constructed, which enables to simulate or to predict the molecule’s properties by the means of computational methods (McCammon, 1987; Ng et al., 2015). However, to eventually test its hypothetical properties, the molecule has to be made physically available through chemical synthesis. The chemical synthesis problem, that is, how to assemble a given molecule with a series of chemical reactions, is a multi-step process with many possible choices at each step and, hence, highly complex. New molecules only come into physical existence if their synthesis route is known, otherwise, they are just an idea. Consequently, several Nobel prizes have been awarded for new reaction mechanisms, such as the the connection of carbons or closing cycles for aromatic structures (Hoffmann, 1982; Corey, 1991). In summary, chemical synthesis is highly complex but crucial for molecule discovery.

To aid in this complex task, chemists have resorted to computer-assisted synthesis planning (CASP) methods to support their discovery of new synthesis paths (Corey & Wipke, 1969; Szymkuć et al., 2016). At the core of every CASP system is a reaction prediction model (Kayala & Baldi, 2012). Early CASP methods were based on rule-based expert systems (Szymkuć et al., 2016) to prioritize chemical reaction to construct a given molecule. More recently, machine learning and deep learning models have been used to learn the rules of chemical reactions and, thereby, enhancing CASP systems (Coley et al., 2018; Segler et al., 2018; Coley et al., 2017). Some machine learning methods directly predict the products of a chemical reaction from the given reactants. In this case, the reaction prediction can be considered as a translation task, in which the reactants represent a sentence in the input language and the products the sentence in the output language (Nam & Kim, 2016; Schwaller et al., 2018a; Liu et al., 2017; Schwaller et al., 2018b). Drawbacks of these methods are their limited interpretability (Fortunato et al., 2020), their potential to produce invalid molecules (Schwaller & Laino, 2019), their lack of being able to directly make use of handcrafted rules, and their insufficient compatibility when trying to integrate them in existing CASP systems. These drawbacks

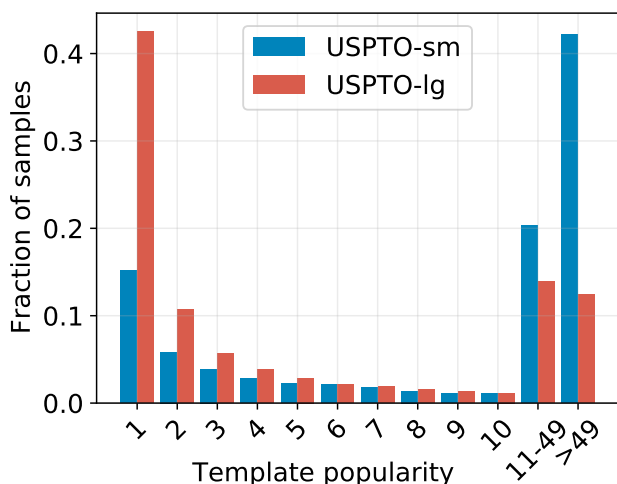


Figure 1. Histogram of reaction template occurrence. The x-axis displays different popularities of reaction templates, concretely in how many chemical reactions a template occurs. The y-axis displays which fraction of samples this popularity category accounts for in the USPTO-sm and USPTO-lg datasets. Both datasets contain reaction templates that occur frequently (right part), but also a high number of samples with reaction templates that occur only once in the dataset (left part). A large fraction of reaction templates both in USPTO-sm and USPTO-lg occur only in a single reaction.

are avoided by template-based reaction prediction models, which rely on a set of transformation rules for molecules, the so-called *reaction templates*. Reaction templates encode both the reactants and products, where reactants are transformed by the chemical reaction to products. However, the selection of the correct reaction template from a large set of possible templates has emerged as a difficult learning problem (Fortunato et al., 2020). Arguably, the first approach using neural networks (NNs) to predict the correct reaction template was by (Wei et al., 2016). In their approach, an NN with one hidden layer predicted the correct template out of a set of 16 expert-encoded templates. This work was extended by Segler & Waller (2017) to predict the correct template out of 8,720 automatically extracted templates from a subset of the Reaxys database. In the seminal work of Segler et al. (2018), an NN model is trained to identify the correct reaction template for a given molecule, where 301,671 reaction templates have been extracted from a large database of reactions. In a CASP system, the model then prioritizes reaction templates to reduce the search space. The database extraction removed rare templates that appeared less than 3 times, which was necessary to have enough training examples for learning, though highly undesired. Somnath et al. (2020) argue that template-based approaches suffer from bad performance, especially for rare reaction templates. Struble et al. (2020) note that ML has not been applied suc-

cessfully for CASP and indicate that especially predictive quality in low-data regimes is lacking. (Baylon et al., 2019) proposed a hierarchical grouping of reaction templates and trained a separate NN for each group of templates. Fortunato et al. (2020) trained on 186,822 reaction templates including those that appear less frequently. This method involves a network pre-training on a large *applicability matrix*, which allows the method to verify whether a reaction template is formally applicable to a set of compounds. Bjerrum et al. (2020) trained two separate NNs. The first NN is trained on the applicability matrix and serves for pre-filtering reaction templates. The second is trained on the reaction dataset, and ranks the reaction templates according to their relevance. Template-based methods are the top-performing methods for reaction prediction (Dai et al., 2020). The drawback of template-based methods is that even if the correct reaction template is selected, it might be applicable to more than one location in the molecule, which can yield ambiguous solutions. Furthermore, reaction templates have to be first extracted from a reaction database or designed by a human expert. Despite these drawbacks, template-based approaches can be favored due to their interpretability. For this reason, template-based approaches are a particularly good match for software tools for chemists (Fortunato et al., 2020). Template-based machine learning methods advanced reaction prediction and reached a top-100 accuracy of 82.2% on the established benchmarking data set USPTO-sm¹ (Wei et al., 2016; Fortunato et al., 2020). However, for many templates only few examples are available in the training set (see Figure 1) which makes accurate predictions difficult (Fortunato et al., 2020). Furthermore, the current methods (Wei et al., 2016; Fortunato et al., 2020) do not learn representations of reaction templates, are constrained to the fixed set of reaction templates on which they were trained and cannot predict novel reaction templates. The prediction of completely novel reaction templates can be considered as a *zero-shot learning* task, which we also address in this work.

Template-based approaches can be either used in CASP systems for forward synthesis or retrosynthesis. In most cases, chemical synthesis planning and CASP systems are formulated as a retrosynthesis problem in which a molecule of interest is recursively decomposed into less-complex molecules until only readily available precursor molecules remain (Segler et al., 2018). In single-step retrosynthesis, the desired molecule is constructed via precursor molecules that are either already available or must be synthesized as well. Therefore, in general multiple retrosynthesis steps are necessary and at each step a large number of potential reactions have to be considered, which leads to a complex, exponentially large search problem. At each retrosynthetic step, a reverse of a chemical reaction is possible, too, which affects the rate of a reaction. Whether a reaction has a

¹In other works, this data set is also called USPTO-50k

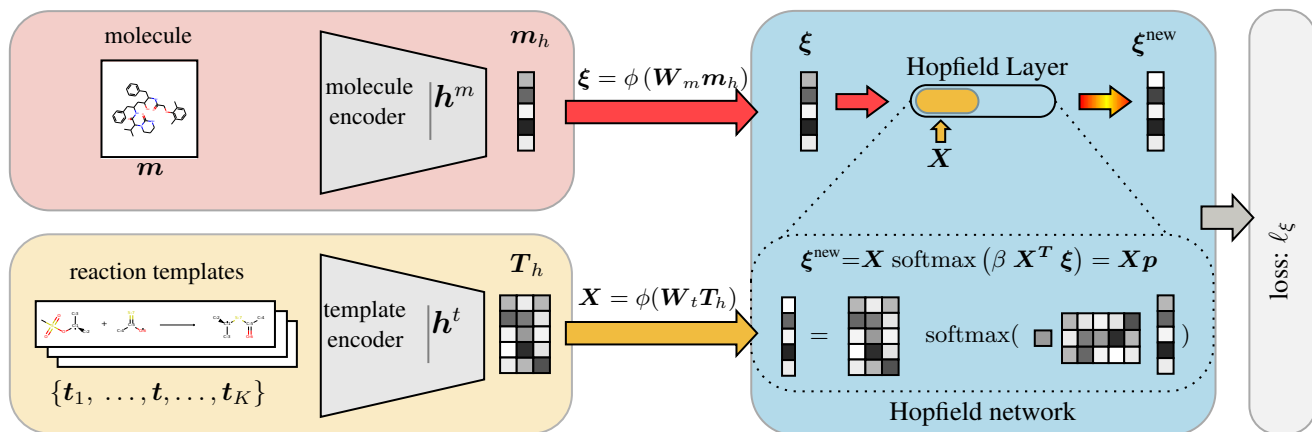


Figure 2. Simplified schematic representation of our approach. Standard approaches only encode the molecule and predict a fixed set of templates, in our MHN-based approach, the templates are also encoded and transformed to stored-pattern via the template encoder. The Hopfield-layer learns to associate the encoded input molecule, the state pattern ξ , with the memory of encoded templates, the stored patterns X .

sufficiently fast rate must also be taken into account by a reaction predictor (Kayala & Baldi, 2012), which further adds to the complexity of the problem. Overall, chemical synthesis planning faces the challenges of an exponentially large search problem, which is additionally exacerbated by hidden reaction characteristics.

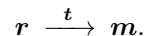
Since CASP systems are mainly improved by new template-based reaction prediction models, we focus on advancing such models by deep learning methods. Template-based methods can predict for each molecule the best suited template without using any template description. This is a classification task, where each template constitutes a class. Alternatively, template-based methods can incorporate template or reaction descriptions and then detect the template description that fits best to a given molecule. This is contrastive learning (Hadsell et al., 2006; Chen et al., 2020), where fitting pairs have to distinguished from non-fitting pairs. The contrastive learning approach enables zero-shot learning, that is, a new molecule can be assigned to a template even if training set molecules were never assigned to this template. We use a contrastive approach which allows for few- and zero-shot learning. We propose a deep learning architecture which exhibits high predictive quality for chemical reactions, concretely single-step retro-synthesis, especially on rare reaction templates, allows for flexible sets of reaction templates, learns representations of both compounds and reaction templates and allows for zero-shot learning. The architecture is based on a *continuous-state modern Hopfield network (MHN)* (Ramsauer et al., 2021; 2020; Widrich et al., 2020), which is a NN with an associative memory in each layer in which patterns are stored. The method learns to retrieve a representation of a reaction template from a memory via associating molecules with

reaction templates. Our method is a contrastive learning approach that associates molecules with templates via an associative memory, which complements previous contrastive learning approaches using a memory (Wu et al., 2018; Misra & Maaten, 2020; He et al., 2020; Tian et al., 2020). With this novel architecture, our method is able to

- generalize across reaction templates and thereby predict templates not seen during training, commonly referred to as zero-shot inference
- exchange the set of templates without the need for retraining
- theoretically store exponentially many patterns (with the size of the association-dimension)
- improve predictive performance, especially for low popularity templates on the USPTO-sm and USPTO-lg data set

2. Template-based retrosynthesis and reaction prediction

In a template-based approach, a chemical reaction is viewed as a tuple (r, t, m) , where r represents a set of reactants, m represents a product molecule and t represents a reaction template that transforms the former into the latter,



The template t is an element of a set of unique reaction templates is $t \in T = \{t^k\}_{k=1}^K$.

2.1. Single-step retrosynthesis

The goal in single-step retrosynthesis is to find a set of molecules that react to a given product. We will also call this task *backward reaction prediction*. Template-based approaches split this task into a two-step procedure. In the first step, relevant reaction templates have to be identified. As molecules can often be synthesized via different reactions there might be multiple correct solutions. A simple attempt to solve this problem would be to check if the product side of a template matches, i.e. is a subgraph of, the molecule of interest. However, this does not consider the context of the whole molecule and other moieties within it, that might conflict with the reaction encoded by the template (Segler & Waller, 2017, Fig. 1). Also, the subgraph matching process is slow, which makes it impractical in planning algorithms. In the second step, this template has to be applied to the given product molecule to infer the reactants. This is not trivial as the template might be applicable in multiple locations. In this study, we focus on the first task only, which in the following we call *backward template prediction*.

The backward template prediction task is defined as follows. Given a product molecule \mathbf{m} a model has to predict templates \mathbf{t} that can be used to synthesize it. As mentioned above, the answer here is not unique which makes evaluation non-trivial. For simplification, \mathbf{m} is often assumed to be a single product molecule (Dai et al., 2020). However, also multiple product molecules could be treated via multiple instance learning (Dietterich et al., 1997; Widrich et al., 2020).

2.2. Reaction prediction

In reaction prediction, the task is to predict the product molecule that will be formed given a set of reactants. As for single-step retrosynthesis, template-based approaches are again two-step procedures. As previously, we only consider template prediction and dismiss the task to identify where it should be applied. Thus, the product information is disregarded and the task is to predict the template \mathbf{t} from the set of reactants \mathbf{r} . We call this task *forward template prediction*.

2.3. Motivation of our approach

We next motivate our method in the backward template prediction setting as it allows for easier notation, but the forward case is analogous. Previous methods (Wei et al., 2016; Fortunato et al., 2020) predict templates using

$$\hat{\mathbf{y}} = \text{softmax}(\mathbf{W} \mathbf{h}^m(\mathbf{m})), \quad (1)$$

where $\mathbf{h}^m(\mathbf{m})$ is neural network that maps a molecule representation to a vector of size d , which we call *molecule encoder*. Via the multiplication with $\mathbf{W} \in \mathbb{R}^{K \times d}$ a score for each template $\mathbf{t}_1, \dots, \mathbf{t}_K$ is obtained. These scores are

then normalized using the softmax function which yields the vector $\hat{\mathbf{y}} \in \mathbb{R}^K$. This approach leads to a multi-class classification task, where a molecule is classified to one of the K classes, each corresponding to a template. However, different templates are viewed as different categories, therefore neither the template descriptions nor similarities between templates are utilized.

We resort to a contrastive learning approach, which uses template descriptions to identify for a molecule a fitting template. Thus, we exploit the descriptions of templates and their mutual similarities. This approach allows for few-shot learning since the classification of a molecule to a template, to which only few molecules have been assigned during training, can be learned via similarities between template descriptions. In particular, we enable zero-shot learning since molecules can be assigned to templates that were not present in the training set. Instead of learning the rows of \mathbf{W} individually, we map each template to a vector of size d using a function \mathbf{h}^t called *template encoder*, and concatenate them row-wise to obtain $\mathbf{T}_h = \mathbf{h}^t(\mathbf{T}) \in \mathbb{R}^{K \times d}$. Replacing \mathbf{W} in the equation above yields

$$\hat{\mathbf{y}}_i = \text{softmax}(\mathbf{T}_h \mathbf{h}^m(\mathbf{m})), \quad (2)$$

which associates the molecule \mathbf{m} with each template via the dot product of their representations. In contrast to \mathbf{W} the rows of \mathbf{T}_h are not learned independently and can use structural information about the template. This contrastive learning approach makes generalization across reaction templates possible, which could allow for improved prediction performance, enables prediction for unseen templates and allows adaption of the set of predicted reaction templates without retraining the model. The next section shows how our contrastive learning approach is realized via modern Hopfield networks.

3. Method: Modern Hopfield networks for reaction template prediction

3.1. Modern Hopfield networks

Recently, Ramsauer et al. (2020; 2021); Widrich et al. (2020) introduced Modern Hopfield Networks (MHN), which are well suited for contrastive learning of associations between sets. MHNs generalize Eq. (2) to a more flexible association mapping

$$\hat{\mathbf{y}} = g(\mathbf{h}^m(\mathbf{m}), \mathbf{h}^t(\mathbf{T})), \quad (3)$$

where g is a modern Hopfield network that is explained below.

We use MHNs for reaction template prediction, where the molecule representation is a *state pattern* $\boldsymbol{\xi} \in \mathbb{R}^d$ and the reaction template representations are the *stored patterns*. MHNs are an associative memory that store patterns $\mathbf{X} \in$

$\mathbb{R}^{d \times K^2}$ and iteratively update a *state pattern* to minimize the following energy function:

$$E = -\text{lse}(\beta, \mathbf{X}^T \boldsymbol{\xi}) + \frac{1}{2} \boldsymbol{\xi}^T \boldsymbol{\xi} + \beta^{-1} \log K + \frac{1}{2} M^2, \quad (4)$$

where $\beta > 0$ is a scaling parameter (inverse temperature), lse is the log-sum-exponential function, K is the number of stored patterns, and M is the largest norm across stored pattern. The update rule is:

$$\boldsymbol{\xi}^{\text{new}} = \mathbf{X} \mathbf{p} = \mathbf{X} \text{softmax}(\beta \mathbf{X}^T \boldsymbol{\xi}), \quad (5)$$

where \mathbf{p} is called the vector of *associations*. The update rule converges globally to stationary points of the energy function (Ramsauer et al., 2020; 2021, Theorem 1 and 2).

The update rule Eq. (5) retrieves averages of the vectors \mathbf{x}_k . However, averages of reaction templates are no longer reaction templates. Therefore, we use the softmax \mathbf{p} to retrieve one of the \mathbf{x}_k via drawing from a multinomial distribution determined by \mathbf{p} . Consequently, we are interested in the *probability* ℓ_ξ of drawing a \mathbf{x}_k that fits to $\boldsymbol{\xi}$. The probability ℓ_ξ can still be computed via a slightly modified Hopfield network update, where instead of data \mathbf{x}_k now labels or scores are retrieved. Such an update has been introduced previously and uses stored patterns that are augmented by labels (Ramsauer et al., 2020, p.83ff). The probability ℓ_ξ of drawing a \mathbf{x}_k that fits to $\boldsymbol{\xi}$ can be computed by a modified Hopfield network update:

$$\mathbf{q}_\xi = \mathbf{L} \mathbf{p} = \mathbf{L} \text{softmax}(\beta \mathbf{X}^T \boldsymbol{\xi}), \quad \ell_\xi = \mathbf{1}^T \mathbf{q}_\xi, \quad (6)$$

where $\mathbf{L} \in \mathbb{R}^{K \times K}$ is the diagonal matrix of labels that are zero or one and $\mathbf{1} \in \mathbb{R}^K$ is the vector of ones. In general, \mathbf{L} can be used to include unlabelled data points as stored patterns, where \mathbf{L} is a Gram matrix times a diagonal label matrix to transfer label information from labelled data points to unlabelled data points. $L_{kk} = 1$ means that \mathbf{x}_k fits to $\boldsymbol{\xi}$ and $L_{kk} = 0$ means that \mathbf{x}_k does not fit to $\boldsymbol{\xi}$. In the context of the Hopfield networks, if more than one \mathbf{x}_k fits to $\boldsymbol{\xi}$ then all \mathbf{x}_k that fit to $\boldsymbol{\xi}$ constitute a metastable state. Instead of L_{kk} being equal to zero or one, L_{kk} can give a non-negative score for how well \mathbf{x}_k does fit to $\boldsymbol{\xi}$. In this case ℓ_ξ is the *expected score*.

Properties. MHNs can retrieve a pattern from exponentially many (with the dimension d) stored patterns (Ramsauer et al., 2020; 2021, Theorem 3), which is beneficial for a large number of templates K . Pattern retrieval requires only one update step that coincides with the update of deep learning layer (Ramsauer et al., 2020; 2021, Theorem 4). Furthermore, MHNs are invariant to permutations of the *stored patterns*.

²Note that K in this work corresponds to N in Ramsauer et al. (2020; 2021)

Algorithm 1 MHN for reaction template prediction.

```

# mol_encoder — fully-connected or GNN. Maps to
dimension  $d_m$ .
# template_encoder — fully connected or linear.
Maps to dimension  $d_t$ .
# m_train, t_train — pair of product molecule
and reaction template from training set
# T — set of  $K$  reaction templates including t_train
# d — dimension of Hopfield space

# forward pass
T_h = template_encoder(T) #[d_t, K]
m_h = mol_encoder(m_train) #[d_m, 1]
x_new, p, X = Hopfield(m_h, T_h, dim=d)
p #[K, 1]

# association loss
L = diag(where(T==t_train)) #[K, K]
loss = -log(sum(L@p))
    
```

Hopfield layers. The Hopfield layers offers a flexible environment to enable learning of associations of two sets, in our case molecules and chemical reactions. It includes additional options, for example, layer normalization (Ba et al., 2016), which can be applied on the stored patterns \mathbf{X} and state pattern $\boldsymbol{\xi}$. Additionally, multiple simultaneous projections into the Hopfield space can be performed, which we – in analogy to attention layers in Transformers – called *heads*.

3.2. Model architecture

Our model architecture consists of three main parts. Firstly, we use a molecule encoder function that learns a relevant representation for the task at hand. For this we use a fingerprint-based, e.g. ECFP (Rogers & Hahn, 2010), fully-connected NN, $\mathbf{h}_w^m(\mathbf{m})$ with weights w . The molecule encoder maps a molecule to its representation $\mathbf{m}_h = \mathbf{h}_w^m(\mathbf{m})$ of dimension d_m .

Secondly, we use the reaction template encoder \mathbf{h}_v^t with parameters v to learn relevant representations of templates. Here, we also use a fully-connected NN with *template fingerprints* as input. These are obtained from a template fingerprint function. Details can be found in section . This function is applied to all templates \mathbf{T} and column-wise concatenation the resulting vectors in a matrix $\mathbf{T}_h = \mathbf{h}_v^t(\mathbf{T})$ with shape (d_t, K) .

Finally, the Hopfield layer g_{Hopfield} (Ramsauer et al., 2020; 2021) associates a molecule with all templates in the memory. It does so by using fully-connected layers to map both molecule representations and template representations to a d -dimensional space, we call *Hopfield space*:

$\xi = \phi(\mathbf{W}_m \mathbf{h}_w^m(\mathbf{m}))$ and $\mathbf{X} = \phi(\mathbf{W}_t \mathbf{h}_v^t(\mathbf{T}))$, where \mathbf{W}_m and \mathbf{W}_t are adaptive weight matrices with d rows, and ϕ is an activation function. The Hopfield layer then employs the update rule Eq. (5) through which the updated representation of the product molecule ξ^{new} and the vector of associations \mathbf{p} is obtained.

In this study, we tested fingerprint-based fully-connected networks for the molecule and template encoder. In principle, one could use every vector-valued molecule representation for these component. One could for example use raw fingerprints, graph neural networks (Gilmer et al., 2017) or SMILES/SMARTS-based RNNs (Mayr et al., 2018) or Transformers.

3.3. Loss function and optimization

In a machine learning approach, the parameters of the model are adjusted on a training set of pairs of molecules with known reaction templates (\mathbf{m}, \mathbf{t}) . Given such a training pair (\mathbf{m}, \mathbf{t}) and the set of all templates \mathbf{T} , the model should assign a high value to the template $\mathbf{t}^k \in \mathbf{T}$ that matches with \mathbf{t} .

Our objective is to minimize $-\log(\ell_\xi)$. If L_{kk} is equal to zero or one, $\log(\ell_\xi)$ is the log-likelihood of drawing a fitting \mathbf{x}_k . If only one \mathbf{x}_k fits (exactly one L_{kk} is one), then our objective is equivalent to the cross-entropy (CE) loss for multi-class classification (see Appendix A). A similar choice for loss function would be to use the InfoNCE (Oord et al., 2018) on the representations in Hopfield space (see Appendix A) However, if more \mathbf{x}_l are labeled as fitting, then our objective can be used but CE could not be appropriate. If L_{kk} is a non-negative score for the molecule-template pair, our approach will maximize the expected score.

We train the full architecture end-to-end using stochastic gradient descent on the loss w.r.t. $\mathbf{W}_t, \mathbf{W}_m, \mathbf{w}, \mathbf{v}$ via the AdamW optimizer (Loshchilov & Hutter, 2017). We train our model for a maximum of 100 epochs and then select the best model with respect to the minimum cross-entropy loss on the validation set. Pseudo-code of the forward-pass including the definition of the loss function of our model is presented in Alg. 1.

Regularization. We use dropout regularization in the molecule encoder \mathbf{h}^m as well as for the template encoder \mathbf{h}^t . We employ L2 regularization on the parameters. A detailed list of considered and selected hyperparameters is given in Tab. 4.

Fingerprint filter (FP Filter). We add a post-processing filter to the predictions which works similar to fingerprint-based substructure screening. For each product and template, we calculated a "PatternFingerprint" using rdkit (Lan-drum, 2016). For a template to be applicable every bit set

in the template fingerprint also has to be set in the product fingerprint. This filtering step further increased performance (see Table 2). We chose a fingerprint size of 4096 as we did not observe significant performance gains for larger sizes, as can be seen in Figure 5.

4. Experiments

4.1. Data

All data sets used in this study are derived from the publicly available U.S. patent literature (USPTO) data set by Lowe (2012). It contains 1,808,938 text-mined reaction equations in SMILES notation (Weininger, 1988) and consists of reactions recorded in the years from 1976 to 2016. Reaction conditions and process actions are not included. From this original data, Fortunato et al. (2020) derived two data sets by preprocessing and filtering procedures. The first is referred to as *USPTO-sm* and is derived from USPTO-50k (Schneider et al., 2016). *USPTO-lg* is based on USPTO-410k by Coley et al. (2019b).

Pre-processing. For pre-processing USPTO-sm and USPTO-lg we followed the implementation of Fortunato et al. (2020). The retrosynthetic templates were extracted from the mapped reactions using RDChiral (Coley et al., 2019a) and subsequently filtered according to symmetry, validity, and by checking if application of the template yielded the same result as in the reaction the template originated from. Despite adhering to the original implementation by the authors, our pre-processing resulted in two datasets with slightly different overall statistics of the reaction templates. The roughly 2 million starting reactions decreased to 443,763 samples and 236,053 reaction templates for USPTO-lg (compared to 669,683 samples and 186,822 reaction templates in Fortunato et al. (2020)), and to 40,257 samples and 9,162 reaction templates for USPTO-sm (compared to 32,099 samples and 7,765 reaction templates in Fortunato et al. (2020)). The template popularity within the data sets is shown in Figure 1. It can be seen that 17% of samples occur in a class that has only one sample in USPTO-sm and 43% in USPTO-lg. 66% of reaction templates in USPTO-sm and 80% in USPTO-lg occur only in a single reaction.

To allow for pre-training of the methods, we calculated the applicability matrix. This step is compute intensive (Fortunato et al., 2020), concretely, without parallelization it would take ≈ 36 hours for USPTO-sm and ≈ 330 days for USPTO-lg with a Xeon(R) Gold 6154 CPU @ 3 GHz when applying the template. Note that a full substructure search yields the same results at approximately one-tenth of the compute time. Thus, we made improvement of the code by Fortunato et al. (2020) which increased the efficiency. Finally, we obtained applicability matrices for both USPTO-

sm and USPTO-Ig which hold the information whether a reaction template can be formally applied to a molecule.

Feature extraction. The source molecules are represented as SMILES. We extract a fingerprint representation of the molecules. Different fingerprint-types have been tried out, e.g. folded Morgan fingerprints with chirality (Morgan, 1965) and the hyperparameter selection procedure (see Table 4) selected Morgan fingerprint size of 2 folded to 4096 features.

For the template representation, a similar procedure has been applied. A template consists of multiple enumerated SMARTS-strings. The fingerprint-type for the templates was set to 'rdk'-fingerprint or 'pattern'-fingerprint and calculated for each molecule that the pattern represents. We experimented with multiple ways of combining not just the product side, but also the reactants side to this representation. The fingerprints were calculated for each molecular pattern and a disjunction over reactants as well as products was calculated. The product minus half of the reactant side results in the template-fingerprint as input for the template encoder.³ Optionally, random features were added to the initial representation of frequent templates in order to help to discriminate frequent templates with a high fingerprint similarity. Templates are classified as "frequent" if appear at least a certain number of times, which is determined by the hyperparameter "random template threshold" (see Table 4).

Data splits. We split the data into a training, validation and test set following Fortunato et al. (2020). Here, a stratified split was used to ensure that templates are more equally represented across the splits. The split proportions were 80/10/10% except for templates with fewer than 10 samples, where one random sample was put into the test set, one into the validation set, and the rest into the training set. If only two samples were present, one was put into the test and one into the training set. If only a single sample was available for a template it was randomly placed into the train/validation/test set with an 80/10/10% chance.

4.2. Compared methods

We compare our MHN approach to previously suggested methods.

- **DNN:** A fully-connected network with softmax output, in which each output unit corresponds to a reaction template similar to the one in Segler & Waller (2017).
- **DNN+pretrain:** The same as the above but pre-trained on the applicability of the train set molecules over all

³Additionally we tried the 'structuralFingerprintForReaction' from RDKit which concatenates the disjunction of each side of the reaction but found the weighted combination to perform better

templates, as suggested by Fortunato et al. (2020).

- **Pop+FP filter:** As a simple baseline we rank templates by their popularity in the training set and apply the FP Filter
- **MHN:** Our approach that uses a modern Hopfield network described above

Note that the methods made particular choices about pre-training strategy, the main architecture and a filtering step. In Section 5 we analyze and dissect those choices in detail.

4.3. Evaluation

For evaluation, we use two main concepts, applicability and relevance. We consider a template to be relevant for a molecule if the reaction it encodes can actually be used to synthesize that molecule. We measure a model's ability to prioritize relevant templates using the recorded molecule/template pairs in the test set as ground truth. Top-k accuracy measures the fraction of samples for which the recorded template is among the highest k predictions.⁴ This indicates the ability of the model to put at least one relevant template among the first k. However, this metric is pessimistic due to label sparsity (Platt et al., 2002). Multiple templates might be relevant for a given molecule but reaction data sets usually only indicate one. We mainly report the top-100 accuracy but also use other values of k in Table 2 and the Appendix.

A template is applicable if its product side is a subgraph of the molecule of interest. This however does not ensure that the reaction is actually feasible as it ignores the context of the whole molecule (Segler & Waller, 2017) which differentiates it from relevance.

In practice, a backward template prediction model would first be trained on available training data and then used to rank templates given a molecule of interest. The set of templates can however only be based on the training set or prior knowledge. The inclusion of templates unique to the test set should be viewed only for evaluating template relevance prediction. When solving the entire single-step retrosynthesis task, the inclusion of those templates should be considered train/test leakage since template extraction already requires knowledge of the whole reaction and thus the solution to the problem. We want to note however that when our approach is used in the full forward/backward reaction task the knowledge of the correct template might give it an advantage compared to template-free methods.

⁴We consider equal prediction scores in the edge case as wrong (if they would not all fit into the remaining ranks), in contrast to e.g. scikit-learn implementation which by default ranks ties by their index.

Top-k accuracy measures the fraction of samples for which the correct template is among the top-k predictions. In the USPTO-sm and USPTO-lg benchmarks, usually, the top-100 accuracy is reported. We additionally report top-1 and top-10 accuracy in Table 2 and in the Appendix.

4.4. Training

All models were trained for a maximum of 100 epochs on a Titan V with 12 GB RAM or a P40 with 24 GB RAM using PyTorch 1.6.0 (Paszke et al., 2019). In the case of DNN, only the molecule encoder was trained and a linear layer, projecting from the last hidden layer to the number of templates was added. For pre-training on the applicability matrix, the loss function changes from binary cross-entropy loss. We also experimented with InfoNCE-loss (Oord et al., 2018) on representations in Hopfield space (see Appendix A). Because of fast convergence and slightly better performance and because for the USPTO data sets only a single template is correct for each molecule, we use our proposed loss, which in this case is equivalent to CE-loss.

Hyperparameter selection Hyperparameters were explored via automatic Bayesian optimization procedure for USPTO-sm, as well as manual hyperparameter-tuning. In the former, early stopping was employed. The range of values was selected based on prior knowledge. Some of the important hyperparameters are the beta scaling factor of the Hopfield layer β , the dimension of the association space d , as well as the association-activation function or if the association space should be normalized via layer-norm (Ba et al., 2016). An overview of considered and selected hyperparameters is given in Tab. 4. For all compared methods (see below), we selected their hyperparameters based on the minimal CE-loss on the validation set.

5. Results

Main results. We evaluated all the models on USPTO-sm and USPTO-lg. Table 1 shows the top-100 accuracy on both data sets. The best top-100 accuracy on USPTO-sm is 0.959 ± 0.004 and is achieved by MHNs combined FP Filter. Also on USPTO-lg, MHNs are the best performing method reaching a Top-100 accuracy of 0.724 ± 0.002 . The second best method is a DNN pre-trained on the applicability matrix (Fortunato et al., 2020) outperforming the DNN baseline. As a trivial baseline, we use the popularity of a template in the training set as prediction score combined with FP Filter.

Rare templates and zero-shot learning. Figure 3 shows the top-100 accuracy for different training set template popularity. Here it can be seen that our approach beats the others by an especially large margin on rare templates. Given that a large fraction of the templates in the test set do not

Table 1. Results in terms of top-100 accuracy of different methods on USPTO-sm and USPTO-lg. Error bars represent standard errors and p -values arise from 2-sample test for equality of proportions.

USPTO-sm	Top-100 acc.
MHN+FP Filter (ours)	0.959 ± 0.004
DNN+Pretrain (Fortunato et al., 2020)	$0.858 \pm 0.004^*$
DNN (Segler & Waller, 2017)	$0.765 \pm 0.005^*$
Pop+FP filter (baseline)	$0.531 \pm 0.004^*$
USPTO-lg	
MHN+FP Filter (ours)	0.724 ± 0.002
DNN+Pretrain (Fortunato et al., 2020)	$0.542 \pm 0.002^*$
DNN (Segler & Waller, 2017)	$0.507 \pm 0.002^*$
Pop+FP filter (baseline)	$0.075 \pm 0.000^*$

* p -value $< 1e-16$.

occur in the training set or do so only once, these improvements at rare templates have a large impact on overall performance. Of note, templates that only occur in the test set can be considered as new classes, which renders this problem a zero-shot learning task. For these new classes or reaction templates, a representation is available, which we can exploit with our proposed architecture in order to make accurate predictions.

Learned template representations. Figure 7 shows a t-SNE embedding of both the reaction fingerprints and the learned embeddings. Each point is coloured according to its class as defined in (Schneider et al., 2015). For example, reactions belonging to the type "oxidations" can be distant in the fingerprint space (pink points in the left figure), while in their learned representations are closer (pink points in right figure). Note that our model did not have access to these reaction types.

Analyzing importance of method choices. In our experiments, we have identified three major method variations, a) choice of neural network architecture, DNN or MHN, b) whether a fingerprint filtering step is performed as post-processing, and c) whether a pre-training on the applicability matrix is done. This results in eight possible combinations of choices, which we test on the benchmarking datasets. The upper section of Table 2 shows the predictive performance of these methods. We observe that the columns are approximately sorted from top-to-bottom. In combination with the organization of the method columns, this implies that MHN contributes the most to improved performance, followed by FP Filter and the use of pre-training. Figure 4 shows the top-100 accuracy for different template popularity for all variations similar to Figure 3. Figure 6 shows the top-k accuracy of all methods for different values of k .

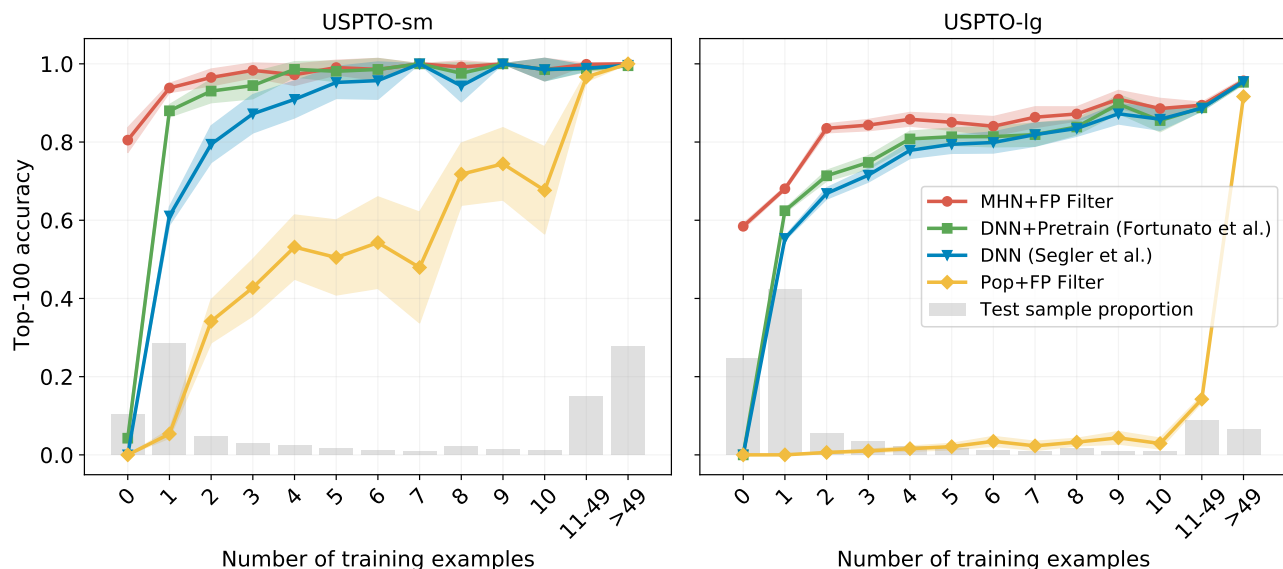


Figure 3. Top-100 accuracy for different template popularity on the USPTO-sm dataset (left) and USPTO-lg (right). The **DNN** is a fully connected NN with softmax output, the method **DNN+Pretrain** is the method proposed in (Fortunato et al., 2020) additionally using pre-training, and **Pop+FP Filter** is a baseline, calculating a full intersection between molecule-fingerprint and template-fingerprint ranked by the popularity in the trainings set. **MHN+FP Filter** is our proposed method using a Hopfield Layer and an FP Filter. The shaded areas represents the 95% confidence interval. The gray bars represent the proportion of samples in the test set. Especially at reaction templates with few examples (left part of x-axis) our method outperforms previous approaches.

Table 2. Top-k accuracy of different method combinations on USPTO-sm and USPTO-lg. The column "Model" refers to which method has been used to rank templates, which is either a fully-connected network (DNN), a modern Hopfield network (MHN), or a naive baseline that ranks templates by their overall popularity (Pop), that is frequency. The column "Filter" specifies if the predictions have been filtered by either using a FP based filter or the applicability matrix (which may in certain cases be computationally infeasible). Pre-train refers to pre-training with applicability information for a fixed number of epochs as proposed by (Fortunato et al., 2020).

Model	Filter	Pretrain	USPTO-sm			USPTO-lg		
			Top-1 acc.	Top-10 acc.	Top-100 acc.	Top-1 acc.	Top-10 acc.	Top-100 acc.
DNN	-	✗	0.381 ^a	0.641 ^a	0.765 ^a	0.160 ^b	0.357 ^b	0.507 ^b
DNN	-	✓	0.385 ^a	0.691 ^a	0.858 ^a	0.208 ^b	0.417 ^b	0.542 ^b
DNN	FP	✗	0.390 ^a	0.676 ^a	0.846 ^a	0.171 ^b	0.381 ^b	0.536 ^b
DNN	FP	✓	0.389 ^a	0.712 ^a	0.906 ^a	0.215^b	0.430 ^b	0.560 ^b
MHN	-	✗	0.399 ^a	0.757 ^a	0.919 ^a	0.167 ^b	0.436 ^b	0.714 ^b
MHN	-	✓	0.404^a	0.762 ^a	0.918 ^a	0.167 ^b	0.435 ^b	0.714 ^b
MHN	FP	✗	0.405^a	0.787^a	0.959^a	0.169 ^b	0.442^b	0.724^b
MHN	FP	✓	0.413^a	0.788^a	0.957^a	0.170 ^b	0.441^b	0.723^b
Pop	-		0.000 ^a	0.086 ^a	0.289 ^a	0.001 ^b	0.008 ^b	0.035 ^b
Pop	FP		0.015 ^a	0.176 ^a	0.531 ^a	0.003 ^b	0.019 ^b	0.075 ^b
Pop	App ^c		0.094 ^a	0.396 ^a	0.803 ^a	0.011 ^b	0.051 ^b	0.165 ^b
DNN	App ^c	✓	0.394 ^a	0.727 ^a	0.952 ^a	0.221 ^b	0.438 ^b	0.569 ^b
MHN	App ^c	✗	0.418 ^a	0.833 ^a	0.993 ^a	0.175 ^b	0.456 ^b	0.743 ^b

^a width of 95% confidence interval < 0.013.

^b width of 95% confidence interval < 0.004.

^c the applicability filter is usually computationally infeasible and, thus, not considered for benchmarking.

The lower part of Table 2 shows the performance of the popularity baseline. The non-negligible performance gain caused by FP filter led us to the question which performance values could potentially be reached with a better filter. To find the upper bound for the performance of a filter, we used the applicability matrix as an optimal filter together with the best MHN and DNN models. This resulted in further accuracy gains, notably MHNs with an applicability filter reached a top-100 accuracy of 0.993, which may motivate an investigation of other fingerprint types to use in the filter. We want to note that these values might be considered as over-optimistic as the applicability filter is expensive to compute.

6. Special cases and related work

The models by Wei et al. (2016), Segler & Waller (2017), and Fortunato et al. (2020) of a fully connected network with softmax output is a special case of our approach. This model is recovered from our model under the following conditions a) one-hot encoding of reaction templates, b) the matrices W_t and W_m are the identity matrices, c) the Hopfield network is constrained to a single update, d) the scaling parameter $\beta = 1$, e) layer norm learns zero mean and unit variance and does not use its adaptive parameters, f) the activation function ϕ is the linear function.

The update-rule of our MHN can be interpreted as the attention mechanism of a Transformer network (Vaswani et al., 2017) as previously shown (Widrich et al., 2020; Ramsauer et al., 2021). From the perspective of attention, our method can be viewed as learning to attend to a memory of reaction templates.

Our approach also has parallels to the recently proposed CLIP algorithm (Radford et al., 2021) which contrastively learns representations of instances from the imaging and the text-domain. The image representation has to identify the correct text representation from a randomly drawn set of text representations, and vice versa. In our MHN approach, we learn a molecule representation to identify the correct reaction template representation from a memory of template representations. Several works focus on learning molecular representations with contrastive approaches (Wang et al., 2021; Fang et al., 2021), however, not learning to contrast reaction templates and molecules.

7. Discussion and conclusion

We have introduced a new Deep Learning architecture for reaction template prediction. The architecture is based on a modern Hopfield network and comprises a molecule and a reaction template encoder network. The latter enables generalization across templates which enables zero-shot learning and improves few-shot learning. Our architecture

outperforms previous methods on the established benchmarks USPTO-Ig and USPTO-sm, which can mainly be attributed to the improved performance on rare templates. The fingerprint-based filter we suggested improved performance and can easily be integrated into existing models.

Although the performance of our current model is probably constrained by the limited coverage of chemical space by the USPTO datasets (Yang et al., 2019), we expect that the performance improvements will translate to larger data sets, such as in-house data sets of pharmaceutical companies. Furthermore, we hope that our approach will be used to improve CASP systems or synthesis-aware generative models (Bradshaw et al., 2019; Renz et al., 2020).

Acknowledgements

The ELLIS Unit Linz, the LIT AI Lab, the Institute for Machine Learning, are supported by the Federal State Upper Austria. IARAI is supported by Here Technologies. We thank the projects AI-MOTION (LIT-2018-6-YOU-212), DeepToxGen (LIT-2017-3-YOU-003), AI-SNN (LIT-2018-6-YOU-214), DeepFlood (LIT-2019-8-YOU-213), Medical Cognitive Computing Center (MC3), PRIMAL (FFG-873979), S3AI (FFG-872172), DL for granular flow (FFG-871302), ELISE (H2020-ICT-2019-3 ID: 951847), AIDD (MSCA-ITN-2020 ID: 956832). We thank Janssen Pharmaceutica (MaDeSMart, HBC.2018.2287), Audi.JKU Deep Learning Center, TGW LOGISTICS GROUP GMBH, Silicon Austria Labs (SAL), FILL Gesellschaft mbH, Anyline GmbH, Google, ZF Friedrichshafen AG, Robert Bosch GmbH, UCB Biopharma SRL, Merck Healthcare KGaA, Software Competence Center Hagenberg GmbH, TÜV Austria, and the NVIDIA Corporation.

References

- Ba, J. L., Kiros, J. R., and Hinton, G. E. Layer normalization. *arXiv preprint arXiv:1607.06450*, 2016.
- Baylon, J. L., Cilfone, N. A., Gulcher, J. R., and Chittenden, T. W. Enhancing retrosynthetic reaction prediction with deep learning using multiscale reaction classification. *Journal of Chemical Information and Modeling*, 59(2):673–688, 2019.
- Bjerrum, E. J., Thakkar, A., and Engkvist, O. Artificial Applicability Labels for Improving Policies in Retrosynthesis Prediction. *ChemRxiv preprint*, 5 2020.
- Bradshaw, J., Paige, B., Kusner, M. J., Segler, M. H., and Hernández-Lobato, J. M. A model to search for synthesizable molecules. *arXiv preprint arXiv:1906.05221*, 2019.
- Chen, T., Kornblith, S., Norouzi, M., and Hinton, G. A

- simple framework for contrastive learning of visual representations. In *International conference on machine learning*, pp. 1597–1607. PMLR, 2020.
- Coley, C. W., Rogers, L., Green, W. H., and Jensen, K. F. Computer-assisted retrosynthesis based on molecular similarity. *ACS Central Science*, 3(12):1237–1245, 2017.
- Coley, C. W., Green, W. H., and Jensen, K. F. Machine learning in computer-aided synthesis planning. *Accounts of chemical research*, 51(5):1281–1289, 2018.
- Coley, C. W., Green, W. H., and Jensen, K. F. Rdkchiral: An rdkit wrapper for handling stereochemistry in retrosynthetic template extraction and application. *Journal of Chemical Information and Modeling*, 59:2529, 2019a.
- Coley, C. W., Jin, W., Rogers, L., Jamison, T. F., Jaakkola, T. S., Green, W. H., Barzilay, R., and Jensen, K. F. A graph-convolutional neural network model for the prediction of chemical reactivity. *Chemical Science*, 10(2):370–377, January 2019b.
- Corey, E. and Wipke, W. Computer-assisted design of complex organic syntheses. *Science*, 166(3902):178–192, October 1969.
- Corey, E. J. The logic of chemical synthesis: multistep synthesis of complex carbogenic molecules (nobel lecture). *Angewandte Chemie International Edition in English*, 30(5):455–465, 1991.
- Dai, H., Li, C., Coley, C. W., Dai, B., and Song, L. Retrosynthesis prediction with conditional graph logic network. *arXiv preprint arXiv:2001.01408*, 2020.
- Dietterich, T. G., Lathrop, R. H., and Lozano-Pérez, T. Solving the multiple instance problem with axis-parallel rectangles. *Artificial intelligence*, 89(1-2):31–71, 1997.
- Fang, Y., Yang, H., Zhuang, X., Shao, X., Fan, X., and Chen, H. Knowledge-aware contrastive molecular graph learning. *arXiv preprint arXiv:2103.13047*, 2021.
- Fortunato, M. E., Coley, C. W., Barnes, B. C., and Jensen, K. F. Data augmentation and pretraining for template-based retrosynthetic prediction in computer-aided synthesis planning. *Journal of Chemical Information and Modeling*, 60(7):3398–3407, 2020.
- Gilmer, J., Schoenholz, S. S., Riley, P. F., Vinyals, O., and Dahl, G. E. Neural message passing for quantum chemistry. In *International Conference on Machine Learning*, pp. 1263–1272. PMLR, 2017.
- Hadsell, R., Chopra, S., and LeCun, Y. Dimensionality reduction by learning an invariant mapping. In *2006 IEEE Computer Society Conference on Computer Vision and Pattern Recognition (CVPR'06)*, volume 2, pp. 1735–1742. IEEE, 2006.
- He, K., Fan, H., Wu, Y., Xie, S., and Girshick, R. Momentum contrast for unsupervised visual representation learning. In *IEEE/CVF Conference on Computer Vision and Pattern Recognition (CVPR)*, 2020.
- Hoffmann, R. Building bridges between inorganic and organic chemistry (nobel lecture). *Angewandte Chemie International Edition*, 21(10):711–724, 1982.
- Kayala, M. A. and Baldi, P. Reactionpredictor: prediction of complex chemical reactions at the mechanistic level using machine learning. *Journal of Chemical Information and Modeling*, 52(10):2526–2540, 2012.
- Landrum, G. Rdkit: Open-source cheminformatics software. 2016.
- Liu, B., Ramsundar, B., Kawthekar, P., Shi, J., Gomes, J., Nguyen, Q. L., Ho, S., Sloane, J., Wender, P., and Pande, V. S. Retrosynthetic reaction prediction using neural sequence-to-sequence models. *CoRR*, abs/1706.01643, 2017.
- Lombardino, J. G. and Lowe, J. A. The role of the medicinal chemist in drug discovery—then and now. *Nature Reviews Drug Discovery*, 3(10):853–862, 2004.
- Loshchilov, I. and Hutter, F. Fixing weight decay regularization in adam. *CoRR*, abs/1711.05101, 2017.
- Lowe, D. M. Extraction of chemical structures and reactions from the literature (doctoral thesis). 10 2012.
- Mayr, A., Klambauer, G., Unterthiner, T., Steijaert, M., Wegner, J. K., Ceulemans, H., Clevert, D.-A., and Hochreiter, S. Large-scale comparison of machine learning methods for drug target prediction on chembl. *Chemical science*, 9(24):5441–5451, 2018.
- McCammon, J. A. Computer-aided molecular design. *Science*, 238(4826):486–491, 1987.
- Misra, I. and Maaten, L. v. d. Self-supervised learning of pretext-invariant representations. In *IEEE/CVF Conference on Computer Vision and Pattern Recognition (CVPR)*, 2020.
- Morgan, H. L. The generation of a unique machine description for chemical structures—a technique developed at chemical abstracts service. *Journal of Chemical Documentation*, 5:107, 1965.
- Nam, J. and Kim, J. Linking the neural machine translation and the prediction of organic chemistry reactions. *arXiv preprint arXiv:1612.09529*, 2016.

- Ng, L. Y., Chong, F. K., and Chemmangattuvalappil, N. G. Challenges and opportunities in computer-aided molecular design. *Computers & Chemical Engineering*, 81: 115–129, 2015.
- Oord, A. v. d., Li, Y., and Vinyals, O. Representation learning with contrastive predictive coding. *arXiv preprint arXiv:1807.03748*, 2018.
- Paszke, A., Gross, S., Massa, F., Lerer, A., Bradbury, J., Chanan, G., Killeen, T., Lin, Z., Gimelshein, N., Antiga, L., Desmaison, A., Kopf, A., Yang, E., DeVito, Z., Raison, M., Tejani, A., Chilamkurthy, S., Steiner, B., Fang, L., Bai, J., and Chintala, S. Pytorch: An imperative style, high-performance deep learning library. In Wallach, H., Larochelle, H., Beygelzimer, A., d'Alché-Buc, F., Fox, E., and Garnett, R. (eds.), *Advances in Neural Information Processing Systems 32*, pp. 8024–8035. Curran Associates, Inc., 2019.
- Platt, J., Burges, C. J. C., Swenson, S., Weare, C., and Zheng, A. Learning a gaussian process prior for automatically generating music playlists. In Dietterich, T., Becker, S., and Ghahramani, Z. (eds.), *Advances in Neural Information Processing Systems*, volume 14. MIT Press, 2002.
- Radford, A., Kim, J. W., Hallacy, C., Ramesh, A., Goh, G., Agarwal, S., Sastry, G., Askell, A., Mishkin, P., Clark, J., et al. Learning transferable visual models from natural language supervision. *Pre-print*, 1:0, 2021.
- Ramsauer, H., Schäfl, B., Lehner, J., Seidl, P., Widrich, M., Gruber, L., Holzleitner, M., Pavlović, M., Sandve, G. K., Greiff, V., et al. Hopfield networks is all you need. *arXiv preprint arXiv:2008.02217*, 2020.
- Ramsauer, H., Schäfl, B., Lehner, J., Seidl, P., Widrich, M., Gruber, L., Holzleitner, M., Pavlović, M., Sandve, G. K., Greiff, V., Kreil, D., Kopp, M., Klambauer, G., Brandstetter, J., and Hochreiter, S. Hopfield Networks is All You Need. *International Conference on Learning Representations (ICLR)*, 2021.
- Renz, P., Van Rompaey, D., Wegner, J. K., Hochreiter, S., and Klambauer, G. On failure modes in molecule generation and optimization. *Drug Discovery Today: Technologies*, 2020.
- Rogers, D. and Hahn, M. Extended-connectivity fingerprints. *Journal of Chemical Information and Modeling*, 50(5):742–754, May 2010.
- Schneider, N., Lowe, D. M., Sayle, R. A., and Landrum, G. A. Development of a novel fingerprint for chemical reactions and its application to large-scale reaction classification and similarity. *Journal of Chemical Information and Modeling*, 55(1):39–53, 2015.
- Schneider, N., Stiefl, N., and Landrum, G. A. What's what: The (nearly) definitive guide to reaction role assignment. *Journal of Chemical Information and Modeling*, 56(12): 2336–2346, 2016.
- Schwaller, P. and Laino, T. Molecular transformer: A model for uncertainty-calibrated chemical reaction prediction. *ACS Central Science*, pp. 12, 2019.
- Schwaller, P., Gaudin, T., Lanyi, D., Bekas, C., and Laino, T. “found in translation”: predicting outcomes of complex organic chemistry reactions using neural sequence-to-sequence models. *Chemical Science*, 9(28):6091–6098, 2018a.
- Schwaller, P., Laino, T., Gaudin, T., Bolgar, P., Bekas, C., and Lee, A. A. Molecular Transformer for Chemical Reaction Prediction and Uncertainty Estimation. *ACS Central Science*, November 2018b.
- Segler, M. H. and Waller, M. P. Neural-symbolic machine learning for retrosynthesis and reaction prediction. *Chemistry - A European Journal*, 23(25):5966–5971, 2017.
- Segler, M. H., Preuss, M., and Waller, M. P. Planning chemical syntheses with deep neural networks and symbolic ai. *Nature*, 555(7698):604–610, 2018.
- Somnath, V. R., Bunne, C., Coley, C. W., Krause, A., and Barzilay, R. Learning graph models for template-free retrosynthesis. *arXiv preprint arXiv:2006.07038*, 2020.
- Struble, T. J., Alvarez, J. C., Brown, S. P., Chytil, M., Cisar, J., DesJarlais, R. L., Engkvist, O., Frank, S. A., Greve, D. R., Griffin, D. J., Hou, X., Johannes, J. W., Kretsoulas, C., Lahue, B., Mathea, M., Mogk, G., Nicolaou, C. A., Palmer, A. D., Price, D. J., Robinson, R. I., Salentin, S., Xing, L., Jaakkola, T., Green, W. H., Barzilay, R., Coley, C. W., and Jensen, K. F. Current and future roles of artificial intelligence in medicinal chemistry synthesis. *Journal of Medicinal Chemistry*, 63(16):8667–8682, 2020. ISSN 0022-2623. doi: 10.1021/acs.jmedchem.9b02120.
- Szymkuć, S., Gajewska, E. P., Klucznik, T., Molga, K., Dittwald, P., Startek, M., Bajczyk, M., and Grzybowski, B. A. Computer-assisted synthetic planning: The end of the beginning. *Angewandte Chemie International Edition*, 55(20):5904–5937, 2016.
- Tian, Y., Krishnan, D., and Isola, P. Contrastive multiview coding. In Vedaldi, A., Bischof, H., Brox, T., and Frahm, J.-M. (eds.), *European Conference on Computer Vision (ECCV)*, pp. 776–794. Springer International Publishing, 2020.
- Vaswani, A., Shazeer, N., Parmar, N., Uszkoreit, J., Jones, L., Gomez, A. N., Kaiser, Ł., and Polosukhin, I. Attention is all you need. *Advances in Neural Information Processing Systems (NeurIPS)*, 30:5998–6008, 2017.

- Wang, Y., Wang, J., Cao, Z., and Farimani, A. B. Molclr: Molecular contrastive learning of representations via graph neural networks. *arXiv preprint arXiv:2102.10056*, 2021.
- Wei, J. N., Duvenaud, D., and Aspuru-Guzik, A. Neural networks for the prediction of organic chemistry reactions. *ACS Central Science*, 2(10):725–732, 2016.
- Weininger, D. SMILES, a chemical language and information system. 1. introduction to methodology and encoding rules. *Journal of Chemical Information and Modeling*, 28(1):31–36, February 1988.
- Widrich, M., Schäfl, B., Ramsauer, H., Pavlović, M., Gruber, L., Holzleitner, M., Brandstetter, J., Sandve, G. K., Greiff, V., Hochreiter, S., and Klambauer, G. Modern Hopfield Networks and Attention for Immune Repertoire Classification. *Advances in Neural Information Processing Systems (NeurIPS)*, 2020.
- Wu, Z., Xiong, Y., Yu, S. X., and Lin, D. Unsupervised feature learning via non-parametric instance discrimination. In *IEEE/CVF Conference on Computer Vision and Pattern Recognition (CVPR)*, pp. 3733–3742, 2018. doi: 10.1109/CVPR.2018.00393.
- Yang, Q., Sresht, V., Bolgar, P., Hou, X., Klug-McLeod, J. L., Butler, C. R., et al. Molecular transformer unifies reaction prediction and retrosynthesis across pharma chemical space. *Chemical Communications*, 55(81):12152–12155, 2019.

Definition	Symbol/Notation	Dimension
set of reaction templates	\mathbf{T}	set of size K
encoded set of reaction template	\mathbf{T}_h	$d_t \times K$
reactant molecules	\mathbf{r}	
product molecule	\mathbf{m}	
encoded molecule	\mathbf{m}_h	d_m
reaction template	\mathbf{t} or \mathbf{t}_k	
training set pair	(\mathbf{m}, \mathbf{t})	
state pattern	$\boldsymbol{\xi}$	d
stored pattern	\mathbf{x}_k	d
stored pattern matrix	\mathbf{X}	$d \times K$
associations	\mathbf{p}	K
update function of MHN	f	
molecule encoder	\mathbf{h}^m	
reaction template encoder	\mathbf{h}^t	
model function	g	
network parameters of \mathbf{h}^m	\mathbf{w}	
network parameters of \mathbf{h}^t	\mathbf{v}	
parameters of Hopfield layer \mathbf{h}^m	$\mathbf{W}_m, \mathbf{W}_t$	$d \times \text{undef}$
association activation function	ϕ	
number of templates	K	
training set size	N	
dimension of association space	d	

Table 3. Symbols and notations used in this paper.

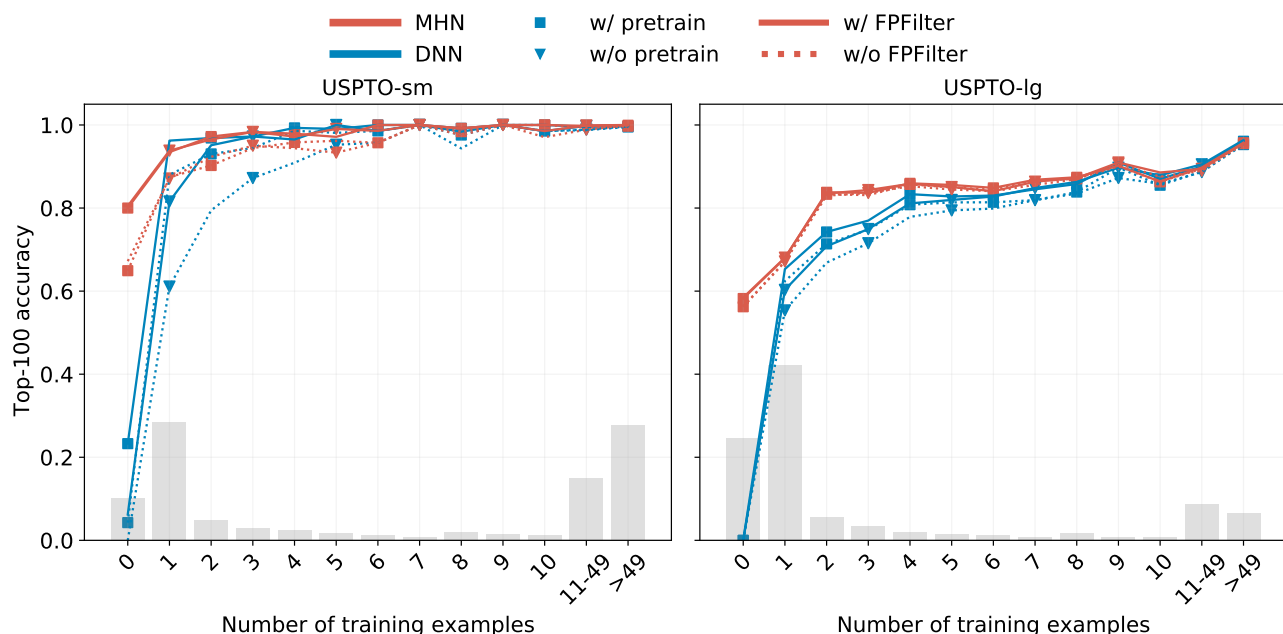


Figure 4. Results of methods with different design elements on the USPTO-sm and USPTO-lg datasets. Each method consists of a combination of the following elements: a) a network MHN or DNN (blue or red line), b) whether pre-training is applied (squares or triangles), and c) whether fingerprint filter is applied for postprocessing (solid or dashed line). These eight possible combinations are displayed as lines with their top-100 accuracy on the y-axis and the different template frequency categories on the x-axis.

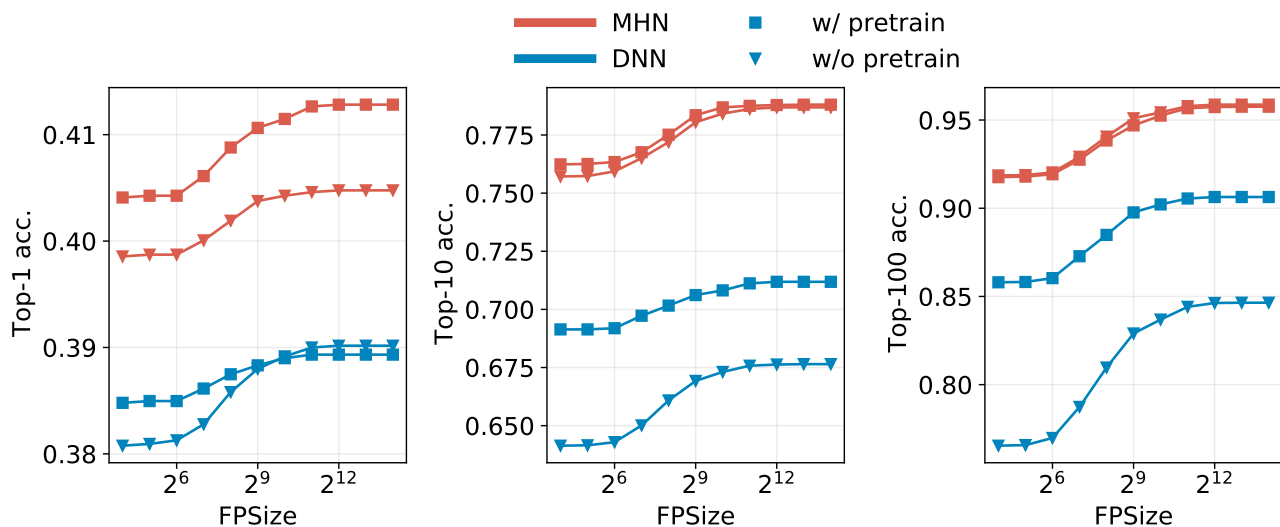


Figure 5. Predictive performance of different methods in dependency of the fingerprint size. Each method consists of a combination of the following elements: a) a network MHN or DNN (blue or red line), and b) whether pre-training is applied (squares or triangles). These four possible combinations are displayed as lines with their top-1, top-10 and top-100 accuracy.

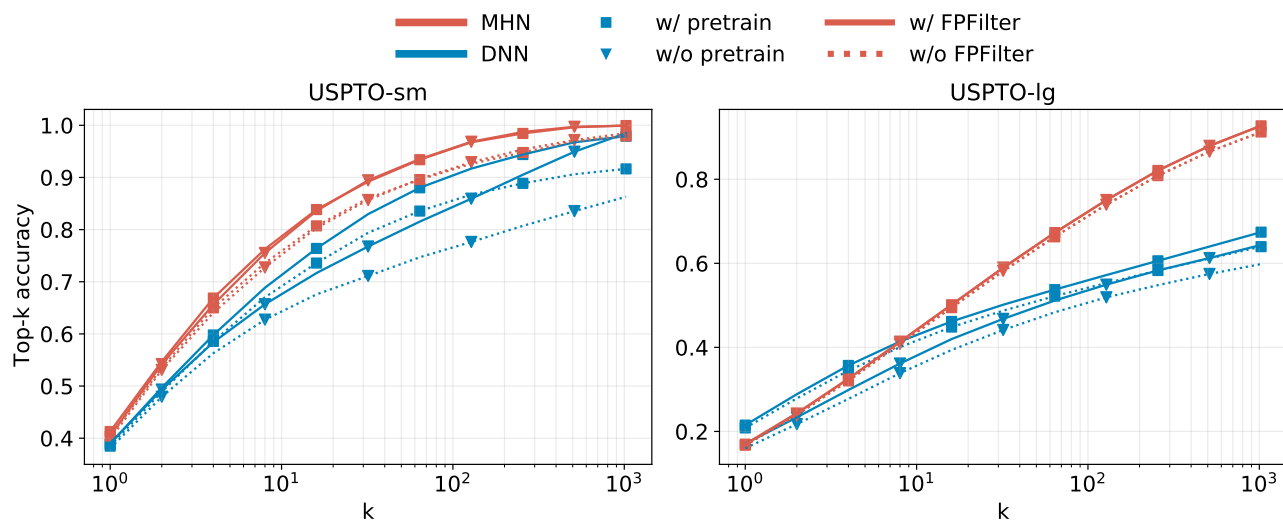


Figure 6. Comparison of methods with respect to their top-k accuracies. Each method consists of a combination of the following elements: a) a network MHN or DNN (blue or red line), b) whether pre-training is applied (squares or triangles), and c) whether fingerprint filter is applied for postprocessing (solid or dashed line). These eight possible combinations are displayed as lines with their k parameter on the x-axis and their top-k accuracy on the y-axis. MHNs provide the best top-k accuracy with k larger or equal 10.

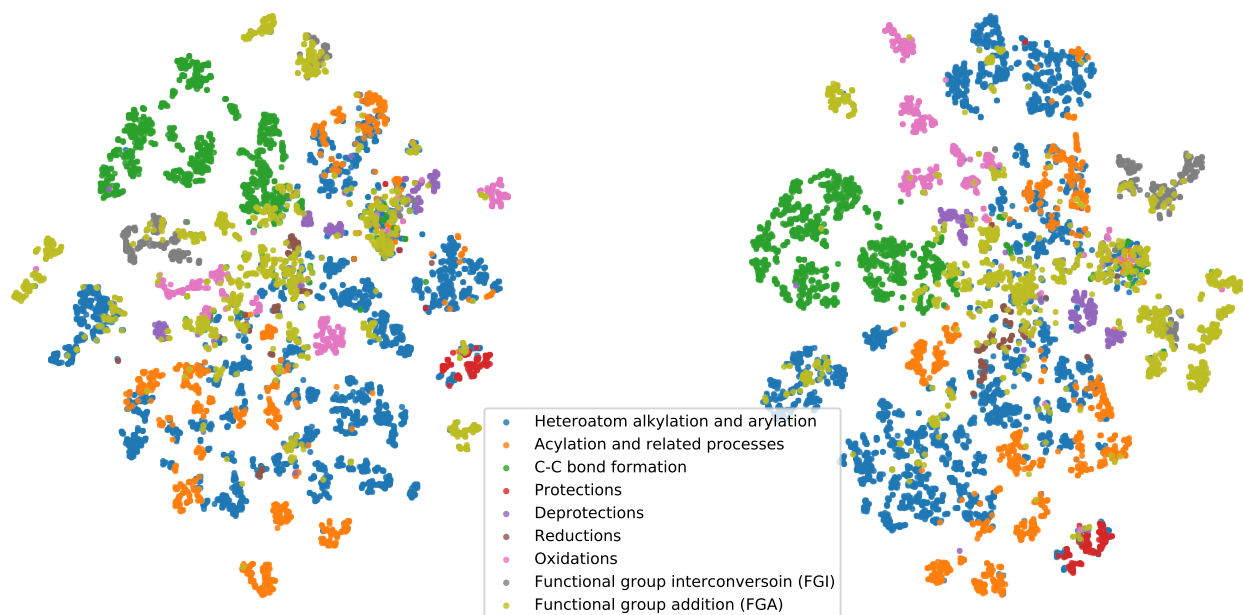


Figure 7. t-SNE downprojection of the reaction template fingerprints (left) and learned representations of reaction templates X (right). The colors represent reaction types of substructure-based expert systems as categorized by (Schneider et al., 2015).

Hyperparam	Values	MHN selected (Sm/Lg)	DNN selected (Sm/Lg)
learning rates	{1e-4, 2e-4, 5e-4, 1e-3}	5e-4 / 1e-4	5e-4 / 2e-4
batch-size	{32, 128, 256, 1024}	1024	256 / 1024
dropout	{0.0, ..., 0.6}	0.2	0.15
<i>molecule encoder</i>			
fingerprint type	{morgan, rdk}	morgan	morgan
fingerprint size	{1024, 2048, 4096}	4096	4096
number of layers	{0, 1, 2}	0	1
layer-dimension	{1024, 2048, 4096}	-	2048
activation-function	{None, SELU, ReLU}	None	ReLU
<i>template encoder</i>			
number of layers	{0, 1, 2}	0	
template fingerprint type	{pattern, rdk}	rdk	
random template threshold	-1, 2, 5, 10, 50	2	
<i>Hopfield layer</i>			
beta	{0.01, ..., 0.3}	0.03	
association activation function	{None, SELU, GeLU, Tanh}	None / Tanh	
normalize state- and stored-pattern	{False, True}	False	
normalize association projection	{False, True}	True	
learnable stored-pattern	{False, True}	False	
hopf-num-layers	{1, 2, 3}	1	
hopf-num-Wm	{1, 2, 3}	1	
hopf-num-Wt	{1, 2, 3}	1	
hopf-FF-activation	{None, SELU, ReLU}	None	
association-dimension d	{32, 64, 512, 1024}	1024	
hopf-num-heads	{1, 6, 12}	1	
<i>Setting-specific-hps</i>			
pre-training epochs	{0,5,10,15,20,25}	10	25 / 5

Table 4. Hyperparameter search-space. All models were trained if applicable for a maximum of 100 epochs using AdamW(Loshchilov & Hutter, 2017) (betas=(0.9, 0.999), eps=1e-8, weight_decay=1e-2, amsgrad=False). A "random template threshold" of -1 corresponds to not adding noise. The fingerprint size for the molecule encoder was always the same as the template encoder. The pre-training learning-rate was also defined by the learning rate, the optimizer remained the same, the loss-function changed to binary cross-entropy loss. "na" stands for non-applicable

A. Loss functions

Cross-entropy. In a simple setting, in which each molecule only has a single correct reaction template in T , a categorical cross-entropy loss is equivalent to the suggested loss. We encode the correct template by a one-hot vector $\mathbf{y} = (0, \dots, 0, 1, 0, \dots, 0)$, where 1 indicates the position of the correct template in the template set $t = t^k$. We then minimize the cross-entropy loss function $\ell_{\text{CE}}(\mathbf{p}, \mathbf{y}) = \text{crossentropy}(\mathbf{p}, \mathbf{y})$ between ground truth \mathbf{y} and the model’s predictions \mathbf{p} for a single pair of the training set and the overall loss is an averages over all such pairs. The corresponding algorithm is given in Alg. 2.

InfoNCE in Hopfield space. An alternative to our proposed loss function could be to use a loss on the retrieved pattern ξ^{new} . The *pattern loss*, could lead to better representations or predictive performance than the cross-entropy loss. The pattern loss measures the cosine similarity of the retrieved pattern with the correct stored patterns with the InfoNCE function (Oord et al., 2018):

$$\ell_p(\xi^{\text{new}}, \mathbf{X}^+, \mathbf{X}^-) = -\text{InfoNCE}(\xi^{\text{new}}, \mathbf{X}^+, \mathbf{X}^-), \quad (7)$$

where \mathbf{X}^+ is the set of representations of correct reaction templates and \mathbf{X}^- is the set of representations incorrect reaction templates, that are contrasted against each other.

Our experiments show that the pattern loss can lead to models with comparable performance to those trained with cross-entropy loss. The according algorithm with pattern loss as alternative loss is shown in Alg. 3.

Algorithm 2 MHN for reaction template prediction - with cross-entropy loss.

```
# mol_encoder — fully-connected or GNN. Maps to dimension  $d_m$ .
# template_encoder — fully connected or linear. Maps to dimension  $d_t$ .
# m_train, t_train — pair of product molecule and reaction template from training set
# T — set of  $K$  reaction templates including t_train
# d — dimension of Hopfield space

# forward pass
T_h = template_encoder(T) #[d_t, K]
m_h = mol_encoder(m_train) #[d_m, 1]
xinew, p, X = Hopfield(m_h, T_h, dim=d)
p #[K, 1]

# association loss
label = where(T==t_train) #[K, 1]
loss = cross_entropy(p, label)
```

Algorithm 3 MHN for reaction template prediction - with InfoNCE loss in Hopfield space.

```
# mol_encoder — fully-connected or GNN. Maps to dimension  $d_m$ .
# template_encoder — fully connected or linear. Maps to dimension  $d_t$ .
# m_train, t_train — pair of product molecule and reaction template from training set
# T — set of  $K$  reaction templates including t_train
# d — dimension of Hopfield space

# forward pass
T_h = template_encoder(T) #[d_t, K]
m_h = mol_encoder(m_train) #[d_m, 1]
xnew, p, X = Hopfield(m_h, T_h, dim=d)

# pattern loss
label = where(T==t_train) #[K, 1]
pos = X[label] #[d, 1]
neg_label = where(T!=t_train) #[K, 1]
neg = X[neg_label] #[d, K-1]
loss = -InfoNCE(xnew, pos, neg)
```
